POLITECNICO DI TORINO
Repository ISTITUZIONALE

Functionalization of transparent conductive oxide electrode for TiO2-free perovskite solar cells

Original
Functionalization of transparent conductive oxide electrode for TiO2-free perovskite solar cells / Topolovsek, P.; Lamberti, F.; Gatti, T.; Cito, A.; Ball, J. M.; Menna, E.; Gadermaier, C.; Petrozza, A.. - In: JOURNAL OF MATERIALS CHEMISTRY. A. - ISSN 2050-7488. - 5:23(2017), pp. 11882-11893. [10.1039/c7ta02405c]

Availability:
This version is available at: 11583/2977477 since: 2023-03-30T10:08:19Z

Publisher:
Royal Society of Chemistry

Published
DOI:10.1039/c7ta02405c

Terms of use:

This article is made available under terms and conditions as specified in the corresponding bibliographic description in the repository

Publisher copyright

(Article begins on next page)

16 April 2024

Optically transparent electrode functionalization for TiO_2-free perovskite solar cells

P. Topolovsek,[a, c] F. Lamberti, [a*] T. Gatti, [b] A. Cito, [a] E. Menna,[b] C. Gadermaier [c, d] and A. Petrozza [a*]

[a] Center for Nano Science and Technology (CNTS), Istituto Italiano di Tecnologia (IIT@PoliMI), Via Pascoli 70/3, 20133 Milano, Italy
[b] Dipartimento di Scienze Chimiche, Università di Padova, via Marzolo 1, 35131 Padova, Italy
[c] Jožef Stefan International Postgraduate School, Jamova 39, 1000 Ljubljana, Slovenia
[d] Jožef Stefan Institute, Jamova 39, 1000 Ljubljana, Slovenia

*Corresponding author(s): Francesco.lamberti@iit.it; annamaria.petrozza@iit.it

Abstract

Here we report on the straightforward modification of an optically transparent electrode with self-assembled siloxane functionalized fullerene molecules. We demonstrate that these molecules form an ultrathin and homogenous electron selective layer on top of the fluorine doped tin oxide (FTO) electrode. We show that fullerene-modified FTO is a robust photoanode for the mixed cation PSCs, reaching over 15% of stabilized power conversion efficiency in a flat junction device architecture by a scalable, low temperature and reliable process.

Introduction

Perovskite solar cells (PSCs) have already exceeded the threshold of 20% stabilized efficiency.[1-3] Most of the efforts now must be focused on the development of device architectures which can guarantee reliable solar cells and a quick industrial scale-up.
Compact anatase titanium dioxide ($cTiO_2$) is normally used as the electron transporting layer (ETL) because it can easily block holes while at the same time it provides a uniform and smooth surface to support perovskite growth.[4] However, it requires high temperature sintering[4] (at least 450 °C) and it is well known to induce electrical instabilities. Such limitations of TiO_2 ETL have been overcome by employing fullerene-based molecules like C60 and its derivative Phenyl-C61-butyric acid methyl ester (PCBM) prepared as thin layers in direct and inverted architectures[5-8], generally together with another hole blocking layer.[9-11] The exact phenomenon leading to such an improvement is still the subject of a debate among experts in the field but it seems quite evident that fullerene derivatives act as a passivating species for interface trap states and improve the charge extraction. They effectively reduce interface recombination and counteract the anion migration that originate from iodine-rich trap states and which amplify the capacitive hysteretic contribution.[5, 7, 8, 12] Deploying fullerene as a stand-alone thin ETL layer between the FTO and perovskite considerably reduces hysteretic behavior through the favorable energy band alignment, resulting in a better electron extraction as well as improved hole blocking properties. Since in the conventional n-i-p configuration the photoactive perovskite is solution processed on top of the ETL, the layer incorporating fullerene or its derivatives needs to be indestructible during further processing with polar aprotic solvents (normally DMF, DMSO or GBL). If

Commentato [1]: Add refs

Commentato [2]: This sbnot needd

Commentato [FL3]: Anna, there's a new ref of Bazan in Nano energy just published highlighting this role. check it, please

this criterion is not opportunely met, the quality and reproducibility of the final device is greatly reduced due to a dissolution of the fullerene film as recently reported in a paper working on fullerene-based ETL engineering.[13] Last, but not the least, fullerene-based derivatives are still quite expensive (roughly 300 eur/g in a scale-up grade) and their synthesis on a large scale for commercial applications remains a major challenge.[14] For this reason, keeping the expensive material consumption as low as possible would be ideal.

The aforementioned problems have been approached so far by covalently binding fullerene molecules to the ETL.[15] Another possible solution would be a direct functionalization of the underlying transparent electrode. One of the most used methodologies for the covalent modification of conductive ceramics such as ITO and FTO is the silanization technique. Silane molecules are generally cheap, easy to handle, and they can be quickly bound to oxygen containing substrate surfaces using standardized recipes either via dip coating, spray coating or CVD, which makes the silanization approach a well-recognized technology in industrial coating applications.[16] The silanized layers show long-term stability to moisture, UV, heat and solvent resistance if opportunely cured, together with a good adhesion to many different substrates.[17, 18] By controlling the humidity condition of the process, it is possible to tune the thickness of the functional layer, from a monolayer (–dry) to a thick cross-linked multilayer.[11]. Of course, this can alter the chemical and electronic properties of the modified substrate as well as the processability and quality of the coating.

Some of us have already demonstrated the possibility of decorating C60 with alkyl siloxane moieties by employing azomethine ylides cycloaddition reactions and subsequently of covalently modifying silica nanoparticles and films with good yields. There are several works in the literature concerning the use of other fullerene-based compounds as electron extraction molecular materials in PSCs; Wojchiechowski and co-workers have recently presented the use of a crosslinked silanized fullerene molecule for creating a thick fullerene layer as an ETL for PSCs.[19] The crosslinking of the spin coated silanized fullerene layer was, in their case, initiated by exposing the layer to vapors of trifluoroacetic acid.

Here we show the possibility of a direct functionalization of the semitransparent electrode by the formation of an electron transporting layer through a silanization-promoted self-assembled ultrathin layer. We use a scalable dip coating technique, which demonstrates the fabrication of a conformal, chemically robust layer resulting in a highly reproducible devices.

Commentato [4]:
It is not clear if there is already a demonstration of this - which means you should add acref, or you are propising it. I have re written assuming that you are introducing a new solution.

Commentato [FL5]: ok, fine

Results and Discussion

In Scheme 1 we report the anchoring mechanism of *N*-[3-(triethoxysilyl)propyl]-2-carbomethoxy-3,4-fulleropyrrolidine, hereby named as **SiI-C60**, on bare FTO. The synthesis of **SiI-C60** has been carried out following a slightly modified procedure with respect to the one previously reported by some of us,[18] allowing to obtain a higher yield, as reported in the Supporting Information (S.I.).[18] Self-assembly of **SiI-C60** on the surface of an FTO electrode was carried out in a low humidity environment (< 10 % R.H.) inside a dry box by a direct immersion of the FTO substrates in a diluted (0.1 mg/ml) **SiI-C60** solution (see S.I. for experimental details). The bare FTO surface is activated by oxygen plasma (O_2 plasma) in order to increase the amount of hydroxyl surface terminated groups, boosting the subsequent covalent attachment of **SiI-C60**. Dry conditions and quick reactions promote the self-assembly mechanism avoiding the development of thick cross-linked coatings. After a final curing step at a relatively low

temperature (110°C), a modified FTO surface is obtained with a covalent self-assembled layer of functionalized C60 molecules, defined from now on as C60-SAL.

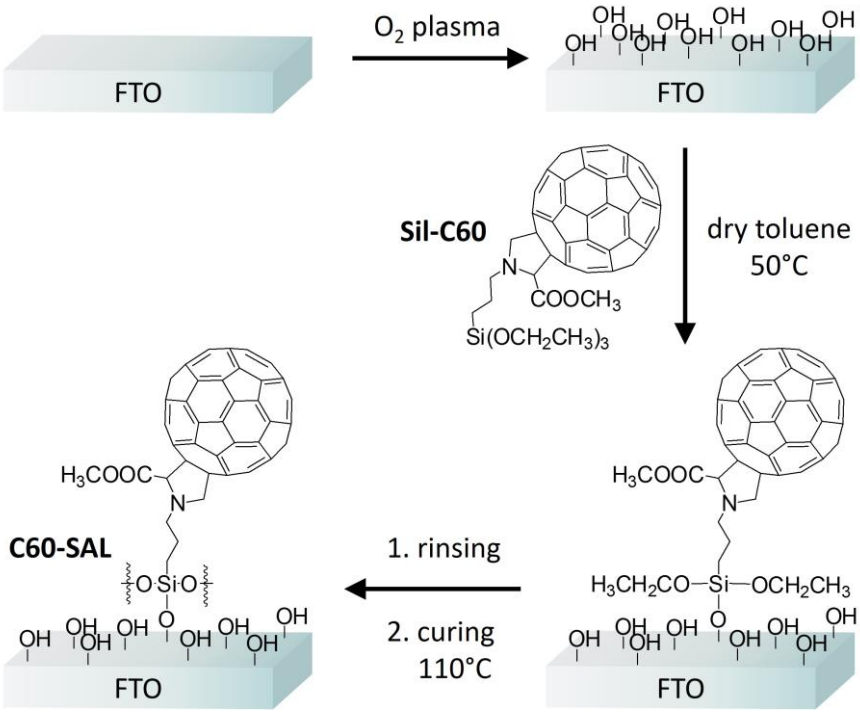

Scheme 1. Illustration of the fullerene self-assembled layer (C60-SAL) fabrication process, involving the covalent anchoring of Sil-C60 on an oxygen plasma-activated FTO substrate.

To gather information on the thickness and surface coverage of FTO by means of C60-SAL we tested this last one– through cyclic voltammetry (CV) and electrochemical impedance spectroscopy (EIS). Experimental details on electrochemical measurements are given in the S.I. ~~first~~ First, the barrier effect towards the diffusion of a charged redox probe in solution after electrode modification has been studied by means of CV (Figure 1a).[20] Here, the positively charged redox probe (ferrocene) is employed to assess the faradic response of a bare FTO electrode and of a functionalized one: the CV clearly shows a quasi-irreversible electrochemical process occurring at the bare FTO surface (ΔE = 0.24V), whereas almost no faradic current is detected when performing CV on C60-SAL under the same conditions. These results suggest a complete modification of the FTO surface by means of **Sil-C60** molecules.[21]

Formattato: Non Apice / Pedice

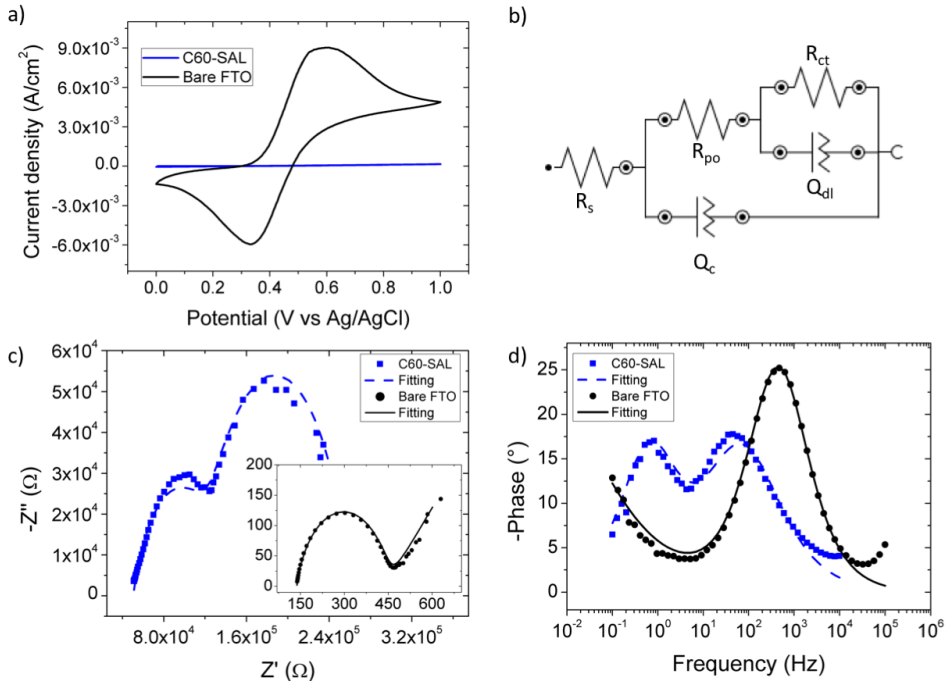

Figure 1. Electrochemical characterization of C60-SAL and bare FTO. a) Cyclic voltammetry (CV) with a ferrocene redox probe (5 mM in ACN solution); b) equivalent circuit for C60-SAL used for the fitting of experimental impedance data in panel c) and d); c) Nyquist plot and d) Bode phase plot of C60-SAL sample; the inset graph in c) shows Nyquist plot of the bare FTO sample. CVs were performed at 25 mV/s (reference electrode: Ag/AgCl; electrolyte: TBATFB 0.1 M in ACN; EIS performed at 0.46 V versus Ag/AgCl with 5 mM ferrocene). Fitted parameters are shown in Table S1 and Table S2.

Stability tests, i.e. several CVs in ACN, confirm chemical and electrical resistance of the modification (Figure S1).

Electrochemical impedance spectroscopy (EIS) also allows to characterize the thickness of the fullerene layer at a good level of approximation. A simple equivalent circuit model is used for fitting the experimental data and is presented in Figure 1b. This circuit is often used for modeling damaged thin coatings in corrosion studies.[22] R_s represents the solution resistance, R_{po} is the ion resistance through the coating (referred to pores or pinholes present within the coating), Q_c is the constant phase element (CPE) related to the intact electrode, R_{ct} is the charge transfer resistance and Q_{dl} is the pseudo-double layer capacitance. Table S1 and Table S2 summarizes all fitted values for different samples. It is possible to determine the thickness of the coating starting from Q_{dl} and to estimate the surface coverage starting from R_{ct}.[23] Therefore, by fitting the experimental data in Figure 1c and 1d a pseudo-capacitance value of C_{dl} = 2.74 uF is obtained that gives a nominal thickness of the silane layer of (3 ± 0.2) nm. Moreover, the surface coverage is estimated to be 99.5% from this analysis. The Nyquist plot in Figure 1c and the Bode phase plot in Figure 1d offer a complete view of the mechanisms involved in the electrochemical reaction at the electrode interface. The bare FTO (black curve in the inset graph in Figure 1c) shows only one semicircle (i.e. a single time constant for the phenomenon) related to a modified Randles cell with a well-defined

Warburg element in the circuit, whereas the C60-SAL modified FTO shows two distinct time constants. Thus, in agreement with the time constants obtained by fitting the electrical circuit model in Figure 1b, two RC contributions are shown (Figure 1d, blue curve): the one at lower frequencies (at about 0.1 Hz) is assigned to the charge transfer reaction at the interface between the solution and the "damaged" coating (i.e. the actual electrochemical reaction taking place at the modified real interface), whereas the higher frequency peak (at about 50 Hz) is due to electrochemical reaction taking place at the intact ideal capacitive coating interface; in addition, the bare FTO resonance peak (black curve in Figure 1d) appears at very high frequencies (about 1 kHz). We can finally conclude that the slower phenomena (i.e. the ones at lower frequencies) occurring at the modified interface are the limiting electrochemical reactions occurring at the modified electrode, thus explaining the lack of faradic current in CV in Figure 1a.

Density Functional Theory (DFT) helps in the rationalization of a model for better describing the topological properties of the C60-SAL. DFT calculations (B3LYP/6-311G**, see S.I. for details) performed on isolated **Sil-C60** show a distance of 1.46 nm between the plane containing the three oxygen atoms bound to Si and the furthest parallel plane containing C atoms on the C60 moiety (see Figure 2a). Based on this estimation and on the outcome of our electrochemical study, which provided a value of 3 nm for the thickness of the fullerene-based layer on top of FTO, we can infer the actual presence of a **Sil-C60** bilayer covering the FTO surface. In Figure 2b, we propose a possible structure for the C60-SAL, where above a first monolayer formed through the covalent binding of **Sil-C60** to the activated FTO surface, a second one forms, through supramolecular self-organization of more Sil-C60 molecules, driven by the formation of strong π-π interactions between fullerene electron clouds.[24]

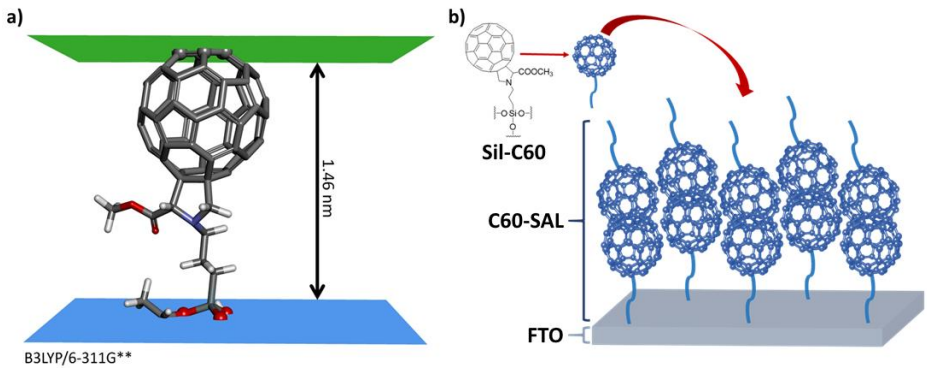

Figure 2. a) Minimized geometry of **Sil-C60**, as calculated through DFT, highlighting the distance between siloxane oxygen atoms and the opposite edge of C60 (see text). b) Schematic representation of the possible bilayer structure of C60-SAL formed by the supramolecular self-organization of **Sil-C60** molecules on top of an activated FTO surface.

We assess the chemical stability of the functionalization by comparing the FTO/C60-SAL substrate with a solution-processed C60 layer as recently presented ~~by~~ by McMeekin *at al.*[25] ~~Wojciechowski *et al.*~~[19] In particular, we measure the water contact angles of the modified substrates before and after the treatment of the substrates in a hot (120 °C) DMF bath, thus simulating potentially damaging conditions for such organic layer during the perovskite processing. This kind of conditions are used, for example, in a hot casting technique or a 2-step perovskite deposition technique using precursor solutions at an

Commentato [6]:
- i guess that to a semicircle is associated a time constant, but First you talk about semi circles then of time constants, this is confusing, be coherent

Commentato [FL7]: fixed

Commentato [8]:
Too confusing..difficult to follow

Commentato [FL9]: revised, check if it is more clear

Formattato: Tipo di carattere: Non Corsivo

Commentato [FL10]: is this the actual ref to compare no? I cannot find this science paper. also, all papers use pcbm spin coated I think, and C60 is tremendoulst used as well. i don't understand why putting them here

Commentato [11]:
Cite the Science from Oxford where the Sn C60 is used and check if there is any other work where the spin coate pcbm or c60 is used

Formattato: Tipo di carattere: Non Corsivo

elevated temperature.[9] The results are summarized in Figure 3 and Table 1, where we show the wettability images and summary of fitted contact angles, respectively.

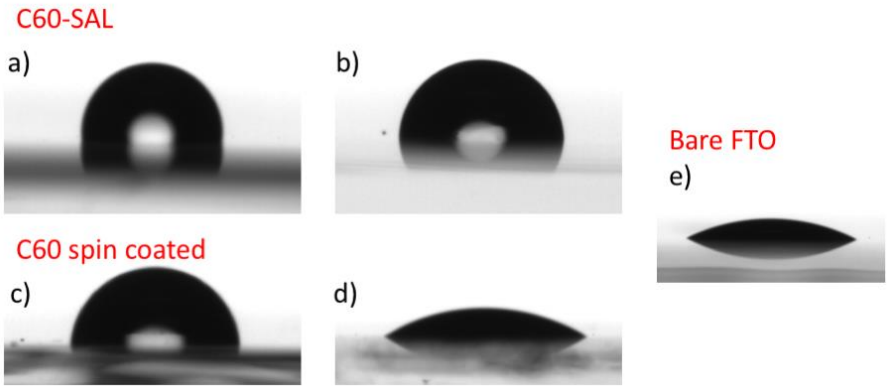

Figure 3. Wettability measurements on FTO modified surfaces with Sil-C60 (C60-SAL) and solution processed fullerene (C60 spin coated). a) and c) refer to as-deposited samples while b) and d) denote samples after 5' immersion in a hot DMF bath; e) refers to a bare FTO as a reference sample.

As highlighted in Table 1, the C60-SAL sample shows high water contact angle before and after the treatment in a hot DMF bath.[26] The spin coated C60 fullerene sample shows reduced contact angle after the treatment, with a value which gets close to that of bare FTO. These results confirm the robust covalent origin of the bond between Sil-C60 and FTO, whereas in the case of spin coated C60 the layer is only weakly interacting with the surface, which results in its almost complete dissolution after hot solvent treatment. Also, the relatively high standard deviation of the contact angle value before DMF treatment for the C60 spin coated sample reveals an intrinsic inhomogeneity of the surface coverage following fullerene processing, that may affect the reproducibility solar cells built upon it.

	Contact angle as deposited (°)	*Contact angle after DMF treatment (°)*	*Relative decrease (%)*
C60-SAL	98 ± 3	85 ± 0.5	11%
C60 spin coated	76 ± 10	19.7 ± 0.5	74%
Bare FTO	20 ± 1	-	-

Table 1. Summary of wettability measurements on samples shown in Figure 3. Error bars refer to at least five repetitive measurements on the same sample in different areas and three different samples per type.

Wettability measurements performed on the C60-SAL sample (Table 1) suggest a high yield of modification throughout the FTO surface with **Sil-C60** molecules with small contact angle deviations over the various spots examined, showing the formation of a conformal and strongly hydrophobic surface. The contact angle on C60-SAL results to be higher than 90°, a value which is significantly far from that of a ~~compact TiO~~c-TiO_2 covered FTO surface (about 22°, not shown) and a plasma treated FTO surface (0°, not shown). The huge change in the wettability of the anode surface due to the presence of

a homogeneously distributed fullerene layer is likely to influence considerably the process of perovskite growth during device realization.

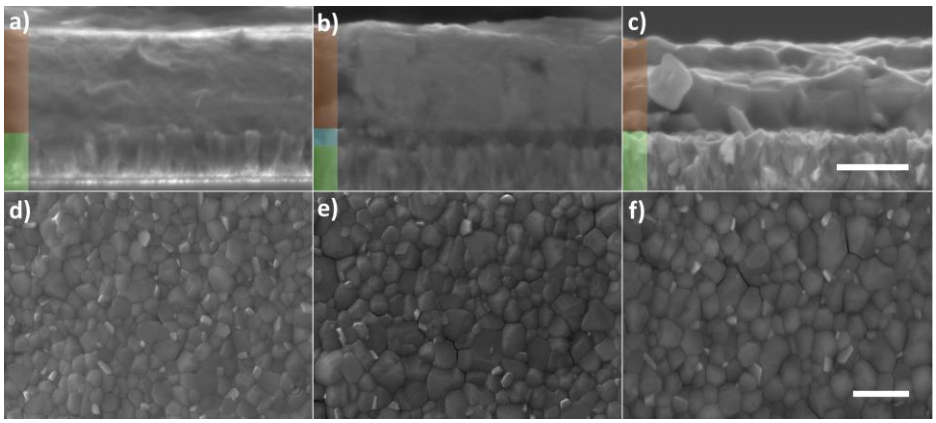

Figure 4. Morphological characterization of perovskite films on various substrates. Cross section (a-c) and surface morphology (d-f) SEM images of perovskite films formed on a bare FTO (a and d), FTO covered with ~~compact TiO~~c-TiO_2 (b and e) and FTO modified by a C60-SAL (c and f). Shaded parts of cross section images mark the FTO (green), ~~compact TiO~~c-TiO_2 (blue) and perovskite layer (brown). The length of a scale bar for cross section images is 500 nm, for surface morphology images 1 um.

In order to understand whether the altered surface properties of various substrates influence the perovskite growth mechanism, we deposited thin perovskite films by spin coating a mixed cation $Cs_{0.175}FA_{0.825}PbI_3$ precursor, using a solvent quenching technique (see Supporting Information for experimental details). We acquired both cross section and surface morphology SEM images of perovskite films deposited on bare FTO (Figures 4a and 4d), FTO covered with ~~compact TiO~~c-TiO_2 (Figures 4b and 4e) and FTO covered with C60-SAL (Figures 4c and 4f). Software analysis of surface morphology SEM images shows a gradual increase of the average grain size from bare FTO (250 nm), to FTO covered with ~~compact TiO~~c-TiO_2 (270 nm) and then to FTO modified by C60-SAL (300 nm). Cross section images revealed less crystalline films formed on a bare FTO and ~~compact TiO~~c-TiO_2 covered FTO, where smaller crystallites are interconnected into a continuous film. In the case of a perovskite layer formed on C60-SAL modified FTO, single perovskite grains proceed~~gress~~ from the top to the bottom of perovskite layer. This increase in the crystallinity may lead to a reduction of charge recombination losses which can happen at grain boundaries~~ries~~. Unfortunately, formation of a perovskite layer on less wettable surfaces leads, in our case, to a reduced thickness of the perovskite layer, which may limit the light absorption (see absorption spectra in Fig S3) and the corresponding photogenerated current.

In Figure 5 we present a correlation between the contact angle measurements and an average perovskite grain size of analyzed films. It seems that an average grain size increases on less wettable surfaces, in agreement to observations reported previously.[27] However, in the referred work 2-step perovskite processing was used, while in our case 1-step with solvent quenching was employed. ~~Here we emphasize that the solvent quenching approach and associated perovskite grain growth dynamics most likely differs from the 2-step perovskite processing and interdiffusion governed grain growth during thermal annealing, as described in the referred work. In the solvent quenching process the crystal size is roughly predefined by the precipitation of the perovskite during the anti-solvent pouring over the substrate, while in the 2-step process~~

Commentato [P12]: Adjusted a bit

Commentato [P13]: Fixed

Commentato [14]:
What is the message here?
Can we say that it is the same mechanism driving the process or not?

Reading it i have the feeling of contrasting statements

You may say that: it has been already shown that ....however, in the solvent quenching Bla-bla-bla

Commentato [FL15]: I agree to Anna comment. you are too much "safe" in explaining useless concepts. try to rewrite the sentecne as Anna suggested, I would use less words.. :D

~~the grain growth proceeds through the constituent interdiffusion during thermal annealing.~~

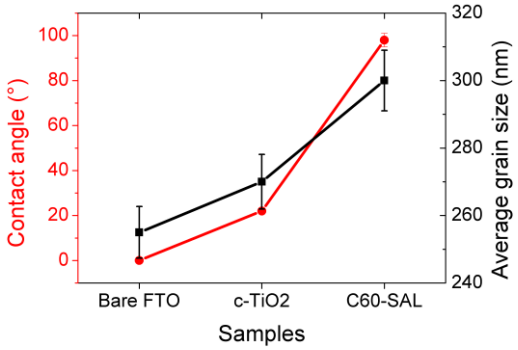

Figure 5. Correlation between the contact angle values and the average perovskite grain size obtained on various substrates.

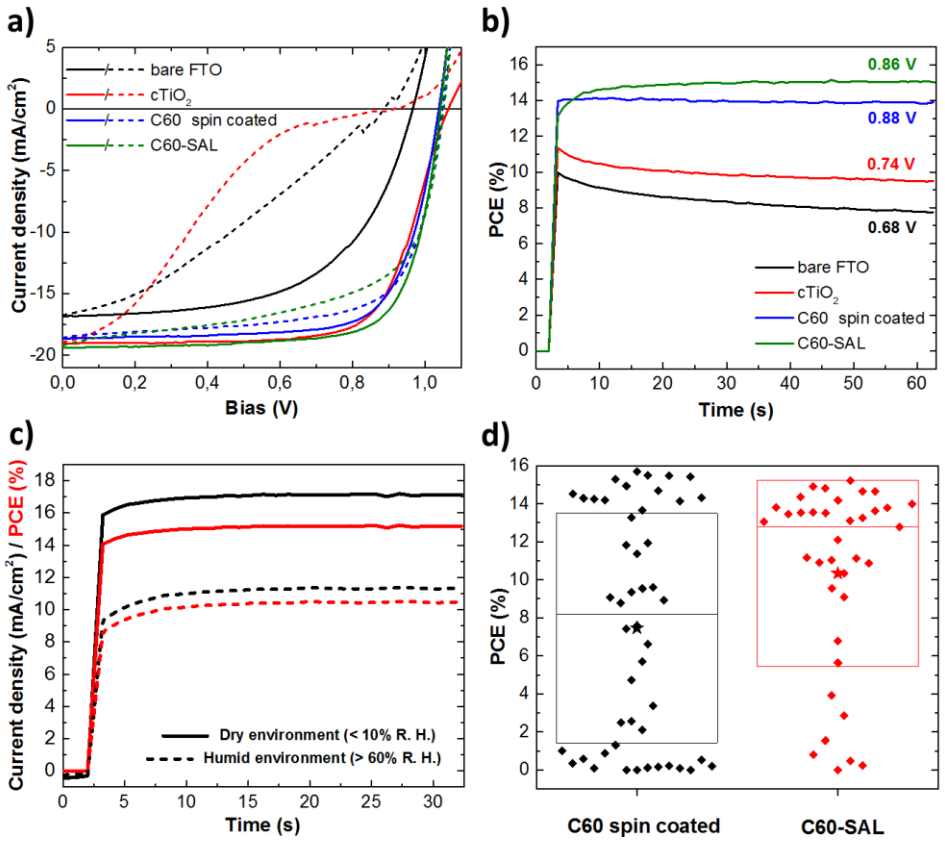

Figure 6. Perovskite solar cell characterization. a) J-V characteristics of devices prepared with no or with various ETLs (as indicated in the legend), presenting backward (solid line) and forward (dashed line) voltage scan direction, measured with a scan rate of 50 mV/s at the intensity of 1 sun. b) Stabilized power conversion efficiency of the best devices measured at the maximum power point. c) Stabilized photocurrents (black lines) and PCEs (red lines) of a typical C60-SAL based device prepared in either dry (solid curves) or humid environment (dashed curves), measured at the maximum power point of 0.76 V and 0.8 V respectively. d) Device statistics on spin coated C60 and C60-SAL as ETLs. A star symbol marks the average value and the box encloses measurements within the standard deviation. The horizontal line inside the box marks the median value. The size of the illuminated area of all devices was 9.38 mm^2.

Perovskite solar cells with C60-SAL, spin-coated C60, ~~compact TiO~~c-TiO_2 and bare FTO as ETLs were fabricated in a direct architecture (i.e. the ETL is deposited directly on the transparent electrode) and tested. The active layer is a mixed cation $Cs_{0.05}FA_{0.75}MA_{0.2}PbBr_{0.3}I_{2.7}$ perovskite, and Spiro-OMeTAD was used as the hole transporting material. The device was finished by a gold cathode. Figure 6a shows current density-voltage characteristics of the best devices. The figures of merit of the solar cells are presented in Table 2. The results show that devices based on FTO covered with spin coated C60 or with C60-SAL show reduced hysteretic behavior during the voltage sweep of 50 mV/s in comparison to a conventional ~~compact TiO~~c-TiO_2 based device or a device without any ETL. It is very well known that the interface between the ~~compact TiO~~c-TiO_2 and perovskite layer is not an efficient electron extraction interface. In order to determine the steady state performance of solar cells regardless of the

voltage scan rate, we tracked the power conversion efficiency (PCE) over time at the maximum power point for each device, as shown in Figure 6b. C60 spin coated and C60-SAL show stable currents with similar performance, reaching up to 15 % PCE as in the case of C60-SAL. The sample with FTO only and with ~~compact TiO~~c-TiO_2 (c-TiO_2) layer show lower starting performances at a maximum power point and a reduction over time.
How effective is the anchoring of the functionalized fullerene molecule depends on the substrate surface termination groups and the environment in which the self-assembly is carried out. To evaluate the preferred treatment conditions we performed the **SiI-C60** self-assembly onto FTO in a dry (< 10% R. H.) or humid (> 60% R.H.) environment. As presented in Figure 6c, devices produced in humid conditions showed decreased performance in terms of stabilized photocurrent and PCE at the maximum power point. We attribute this outcome to a poor bonding of **SiI-C60** in the presence of water in the atmosphere in which the treatment is performed and in the **SiI-C60** solution. High concentration of water molecules in the chemical environment favors the cleavage of Si-O-Si bonds by the formation of patched areas of different thicknesses. Poor charge selectivity in uncovered areas contribute to a higher recombination rate of photogenerated charges nearby the electrode, effectively reducing the extracted photocurrent.[28]
Since the C60-SAL showed a better resistance to dissolution compared to a spin coated C60 and a more uniform surface coverage due to a chemical bonding to the surface, we analyzed the performance of a large ensemble of devices for both configurations, as presented in Figure 6d, in order to evaluate the role of chemical resistance on the reliability of the devices and of the process. As expected PCEs obtained with a spin coated C60 showed large dispersion of results, while devices produced on C60-SAL showed more consistent results, with a better average performance. Although the thickness of the C60-SAL is much lower than the thickness of a spin coated C60 (about 20nm, measured by a profilometer), it acts as a stable electron extraction layer, presenting significant advantage over the spin coated fullerene ETL.

	Bare FTO		*$cTiO_2$*		*C60 spin coated*		*C60-SAL*	
	BWD	FWD	BWD	FWD	BWD	FWD	BWD	FWD
V_{oc} (V)	0.97	0.88	1.06	0.92	1.04	1.05	1.04	1.05
J_{sc} (mA/cm²)	16.8	16.7	19.0	18.9	18.6	18.6	19.4	19.2
FF	0.58	0.31	0.71	0.21	0.73	0.69	0.74	0.60
PCE (%)	10.3	5.1	14.5	3.7	14.3	13.6	15.2	12.4

Table 2: Solar cell parameters obtained from the J-V characteristics presented in a Figure 3a.

Conclusions
We show that functionalized fullerene molecules can covalently bind to a clean, oxygen terminated surface of an FTO electrode, forming a robust, conformal and chemically inert ultrathin self-assembled film. This is enough to act as efficient and reliable electron extracting layer in mixed cation perovskite solar cells, reducing the current-

voltage hysteresis and reaching over 15 % of stabilized PCE. Application of strongly bound fullerene molecules as an interfacial layer not only eliminates the need of any high temperature processing but also significantly reduces the material consumption through the mechanism of self-assembly, which renders this approach much closer to an industrial scale production than any other solution processing technique.

Author contributions.

P.T. and F.L. wrote the manuscript, F.L. performed FTO modification, electrochemical measurements and grains size analysis on SEM images; P.T. prepared the device and performed profilometer and UV-Vis characterization. A.C. performed wettability measurements; T.G. synthesized Sil-C60, E.M. performed DFT calculations and contributed to the supervision of the work, A.P. and F.L. conceived the idea for the project and designed the experiments. All authors reviewed the paper.

Acknowledgment

The research leading to these results has received funding from the European Union Seventh Framework Programme [FP7/2007-2013] under grant agreement 316494, from DESTINY project (Contract No. 316494), from the Italian "Ministero dell'Istruzione, dell'Università e della Ricerca (MIUR) with PRIN project DSSCX (n. 20104XET32) *and from CARIPLO foundation (GREENS project No. 2013-0656 and IPER-LUCE No. 2015-0080).*
We would also like to acknowledge Dr. James Ball for the work on automated solar simulator system and data analysis script and Dr. Andrea Desii for the SEM images.

References

[1] S. D. Stranks and H. J. Snaith, Nat. Nano. 10 (2015) 391-402.
[2] M. Saliba, T. Matsui, J.-Y. Seo, K. Domanski, J.-P. Correa-Baena, M. K. Nazeeruddin, S. M. Zakeeruddin, W. Tress, A. Abate, A. Hagfeldt and M. Gratzel, En. Environ. Sci. 9 (2016) 1989-1997.
[3] W. S. Yang, J. H. Noh, N. J. Jeon, Y. C. Kim, S. Ryu, J. Seo and S. I. Seok, Science 348 (2015) 1234-1237.
[4] D. Bi, W. Tress, M. I. Dar, P. Gao, J. Luo, C. Renevier, K. Schenk, A. Abate, F. Giordano, J.-P. Correa Baena, J.-D. Decoppet, S. M. Zakeeruddin, M. K. Nazeeruddin, M. Grätzel and A. Hagfeldt, Sci. Adv. 2 (2016.
[5] Y. Xing, C. Sun, H. L. Yip, G. C. Bazan, F. Huang and Y. Cao, Nano En. 26 (2016) 7-15.
[6] C.-H. Chiang and C.-G. Wu, Nat. Photon. 10 (2016) 196-200.
[7] J. Xu, A. Buin, A. H. Ip, W. Li, O. Voznyy, R. Comin, M. Yuan, S. Jeon, Z. Ning, J. J. McDowell, P. Kanjanaboos, J.-P. Sun, X. Lan, L. N. Quan, D. H. Kim, I. G. Hill, P. Maksymovych and E. H. Sargent, Nat. Commun. 6 (2015) 7081.
[8] Y. Shao, Z. Xiao, C. Bi, Y. Yuan and J. Huang, Nat. Commun. 5 (2014) 5784.
[9] C. Tao, S. Neutzner, L. Colella, S. Marras, A. R. Srimath Kandada, M. Gandini, M. D. Bastiani, G. Pace, L. Manna, M. Caironi, C. Bertarelli and A. Petrozza, En. Environ. Sci. 8 (2015) 2365-2370.

Formattato: Italiano (Italia)

[10] T. Leijtens, G. E. Eperon, S. Pathak, A. Abate, M. M. Lee and H. J. Snaith, Nat. Commun. 4 (2013) 2885.
[11] A. Baptiste, A. Gibaud, J. F. Bardeau, K. Wen, R. Maoz, J. Sagiv and B. M. Ocko, Langmuir 18 (2002) 3916-3922.
[12] O. Almora, I. Zarazua, E. Mas-Marza, I. Mora-Sero, J. Bisquert and G. Garcia-Belmonte, J. Phys. Chem. Lett. 6 (2015) 1645-1652.
[13] K. Wojciechowski, T. Leijtens, S. Siprova, C. Schlueter, M. T. Hörantner, J. T.-W. Wang, C.-Z. Li, A. K. Y. Jen, T.-L. Lee and H. J. Snaith, J. Phys. Chem. Lett. 6 (2015) 2399-2405.
[14] D. M. Guldi and N. Martin, *Fullerenes: From Synthesis to Optoelectronic Properties*, Springer-Science, 2002.
[15] A. Abrusci, S. D. Stranks, P. Docampo, H.-L. Yip, A. K. Y. Jen and H. J. Snaith, Nano Lett. 13 (2013) 3124-3128.
[16] J. G. Matisons, in *Silicone Surface Science*, eds. J. M. Owen and R. P. Dvornic, Springer Netherlands, Dordrecht, 2012, DOI: 10.1007/978-94-007-3876-8_10, pp. 281-298.
[17] B. Arkles, J. R. Steinmetz, J. Zazyczny and P. Mehta, J. Adhes. Sci. Techn. 6 (1992) 193-206.
[18] A. Bianco, F. Gasparrini, M. Maggini, D. Misiti, A. Polese, M. Prato, G. Scorrano, C. Toniolo and C. Villani, J. Am. Chem. Soc. 119 (1997) 7550-7554.
[19] K. Wojciechowski, I. Ramirez, T. Gorisse, O. Dautel, R. Dasari, N. Sakai, J. M. Hardigree, S. Song, S. Marder, M. Riede, G. Wantz and H. J. Snaith, ACS En. Lett. 1 (2016) 648-653.
[20] F. Lamberti, L. Brigo, M. Favaro, C. Luni, A. Zoso, M. Cattelan, S. Agnoli, G. Brusatin, G. Granozzi, M. Giomo and N. Elvassore, ACS Appl. Mater. Interfaces 6 (2014) 22769-22777.
[21] B. Roose, J.-P. C. Baena, K. C. Gödel, M. Graetzel, A. Hagfeldt, U. Steiner and A. Abate, Nano En., DOI: http://dx.doi.org/10.1016/j.nanoen.2016.10.055 (in press.
[22] R. Zhang, L. Wang and W. Shi, RSC Adv. 5 (2015) 95750-95763.
[23] G. Sánchez-Pomales, L. Santiago-Rodríguez, N. E. Rivera-Vélez and C. R. Cabrera, J. Electroanal. Chem. 611 (2007) 80-86.
[24] S. Zhou, C. Burger, B. Chu, M. Sawamura, N. Nagahama, M. Toganoh, U. E. Hackler, H. Isobe and E. Nakamura, Science 291 (2001) 1944-1947.
[25] D. P. McMeekin, G. Sadoughi, W. Rehman, G. E. Eperon, M. Saliba, M. T. Hörantner, A. Haghighirad, N. Sakai, L. Korte and B. Rech, Science 351 (2016) 151-155.
[26] D. Dattilo, L. Armelao, M. Maggini, G. Fois and G. Mistura, Langmuir 22 (2006) 8764-8769.
[27] C. Bi, Q. Wang, Y. Shao, Y. Yuan, Z. Xiao and J. Huang, Nat. Commun. 6 (2015) 7747.
[28] A. Guerrero, B. Dörling, T. Ripolles-Sanchis, M. Aghamohammadi, E. Barrena, M. Campoy-Quiles and G. Garcia-Belmonte, ACS Nano 7 (2013) 4637-4646.

Formattato: Italiano (Italia)
Formattato: Italiano (Italia)
Formattato: Italiano (Italia)
Formattato: Italiano (Italia)
Formattato: Italiano (Italia)